

Variation of the microstructure and fracture strength of cold isostatically pressed alumina ceramics with the alteration of dewaxing procedures

Nobuhiro Shinohara^a, Masataro Okumiya^a, Tadashi Hotta^b, Kenji Nakahira^b, Makio Naito^{b,*}, Keizo Uematsu^c

^aResearch Center, Asahi Glass Co., Ltd., Hazawa-cho, Kanagawa-ku, Yokohama, 221-8755, Japan

^bJapan Fine Ceramics Center, 2-4-1, Mutsuno, Atsuta-ku, Nagoya 456-8587, Japan

^cDepartment of Chemistry, Nagaoka University of Technology, 1603-1, Kamitomioka-cho, Nagaoka 940-2188, Japan

Received 28 June 1999; received in revised form 30 August 1999; accepted 12 September 1999

Abstract

Influence of the alteration of CIP and dewaxing procedures on the pore structure and the fracture strength of sintered alumina ceramics was examined. Variation of the fracture strength with the process alteration could be explained by the difference in distribution of large pore defects determined by applying the direct observation techniques. Dewaxing, before CIP, varied the strength and fracture behavior of granules and was effective in promoting the uniform powder packing during consolidation, resulting in the high strength of sintered bodies. © 2000 Elsevier Science Ltd. All rights reserved.

Keywords: Al₂O₃; Failure analysis; Mechanical properties; Microstructure-final; Microstructure-prefiring; Pressing

1. Introduction

The manufacturing process exerts a very important influence on the microstructure and properties of ceramic materials. In a given production method, a minor change of processing condition can have a very strong effect on them. In ceramic materials formed through the powder compaction method, large pores responsible for the reduction of fracture strength are often found in sintered bodies.^{1,2} The major source of these large pores can be related to the structure and characteristics of utilized granules.^{3,4} Dimples in granules and the incomplete adhesion between granules result in the formation of void spaces at their center and boundaries in green compacts. These pore defects persist or even grow in sintering, forming fracture origins which cause the degradation of fracture strength of sintered bodies.^{5–9} Controlling both the structure and characteristics of granules as well as the compaction behavior thus becomes an important issue for the reduction in the

concentration and size of pore defects to improve the strength and reliability of ceramic materials.

There are many factors exerting an influence on the structure and characteristics of granules. For example, the structure of granules are changed by the dispersion properties of powder particles in slurry.^{1,3} Their compressive properties are influenced by the ambient temperature and humidity.^{4,12–16} It has been shown that soft and deformable granules are favorable to exhibit high density with better joining between granules and high strength in green bodies.^{12–17} However, the effect of fracture behavior of granules on the compaction and the properties of green and sintered ceramic bodies have not been well understood.

The characteristics and compaction behavior of granules are mainly governed by the added organic binder system, provided that other preparation conditions such as slurry concentration, viscosity, and spray drying conditions, etc. are essentially unchanged. Dewaxing by the heat treatment of granules is, therefore, expected to vary the property of granules and the resultant compaction behavior.

In this study, influence of the heat-treatment of green compacts before and after CIP was investigated on the

* Corresponding author. Tel.: +81-52-871-3500; fax: +81-52-871-3599.

E-mail address: naito@jfcc.or.jp (M. Naito).

variation of structure and fracture strength of sintered alumina ceramics, because the compaction during CIP should still be dominated by the characteristics of granules. Direct observation techniques developed by Uematsu et al. are applied to examine the structure variation in CIPed and sintered bodies,^{10,11} and the relevance of the structural variation to the fracture strength is discussed.

Effect of the heat-treatment of granules on their characteristics was also examined. Fracture strength of granules was measured and the fracture behavior was observed. The results are briefly mentioned in this study to explain the difference in green microstructure.

2. Experimental procedure

The starting material is low-soda alumina (AES-11E, SUMITOMO CHEMICAL Co., Ltd.) with an average particle size of 0.4 μm and a purity of 99.8% containing 300 ppm of MgO as a sintering agent. The granules were prepared according to the procedure shown in the previous reports.^{4–7} Polyvinyl alcohol and wax were added as binders, and the amount of organic components in binders and other additives was controlled to be 0.5 wt% to the weight of alumina powder.

The granules were uniaxially mold pressed into compacts at 10 MPa with a metal mold. The compacts were then divided into two groups. One was CIPed subsequently followed after mold pressing, and dewaxed by heat-treating at 500°C for 5 h in the electric furnace (referred to as AC in the description below). The other was first dewaxed at 500°C, then CIPed for further compaction (referred to as BC). CIPing was carried out at 176 MPa for compacts in both groups. The size of green compacts was 50×60×10 mm. All powder compacts were sintered at 1590°C for 2 h in the electric furnace.

Densities of sintered samples were measured by using Archimedes method in water. Test specimens with the size 3×4×40 mm were cut and ground from the sintered samples for the fracture strength and toughness measurements. The surface of the specimens was finished with a diamond grinding wheel of No. 800. Four point bending strength was measured for specimens according to JIS R1601 by using a universal testing machine with the cross head speed of 0.5 mm/min. The single-edged-precracked beam method was applied to measure the fracture toughness according to JIS R1607.

The structures of green bodies were examined in transmission mode for thinned specimens with the liquid immersion method. For the structural observation of green bodies, the samples were thinned to a tenth of a millimeter thick with grinding paper. A few drops of 1-bromonaphthalene and methyleneiodide were added to make them transparent and to observe the structure in transmission mode. For the structural

observation of sintered bodies, the samples were thinned to the thickness of less than about 50 μm and finished with diamond pastes of 0.5–2 μm . Micrographs were taken on the thinned specimens with transmission mode without adding any immersion liquids. The size and the concentration of pores were examined on the micrographs.

Fracture behavior of a single granule was analyzed by a diametral microcompression testing machine (model PCT-200, Shimadzu, Japan) for both as-granulated and dewaxed granules. Dewaxing was also carried out by heat-treating the granules at 500°C. The strength of the granule was determined according to the procedure shown in the previous report.¹⁸

3. Results

Fig. 1 shows the SEM micrographs taken on the fracture surface of green compacts. The trace of granules is observed in the green compact prepared through AC process. Clearly, the adhesion of granules was improved in the green body in the BC group.

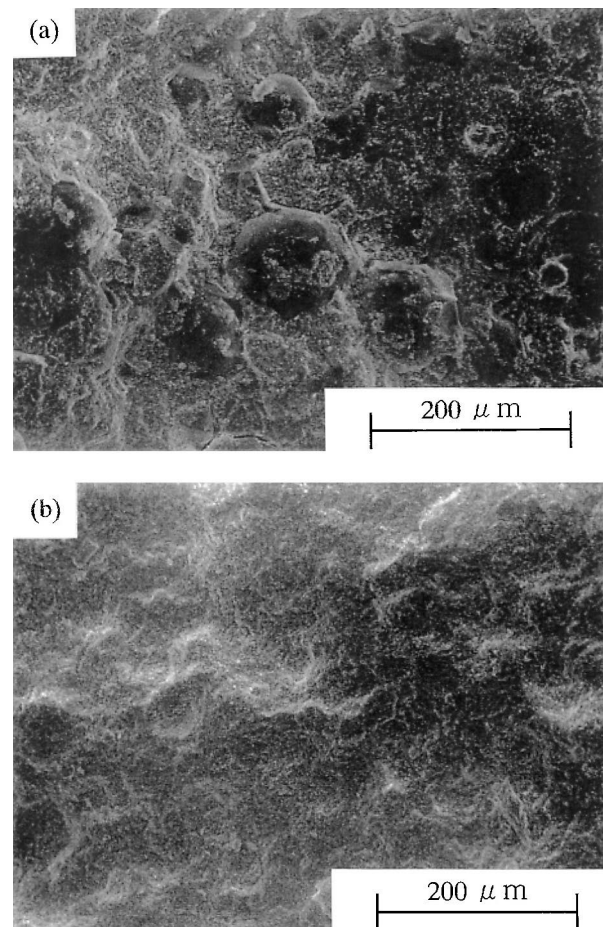


Fig. 1. SEM micrographs taken on the fracture surface of green bodies made through (a) AC and (b) BC processes.

Fig. 2 shows the normal optical micrographs taken with transmission mode with the liquid immersion method for green compacts. Boundaries of granules and pores are visible in both compacts, even in the BC sample. It was very difficult to notice these kinds of pore structures in green compacts by SEM, as shown in Fig. 1. In the optical micrographs, a larger size and population of pores are evident for the green body in the AC group than for the BC. These pores are formed from dimples in granules and void spaces at the boundaries of granules.

Fig. 3 shows the SEM micrographs taken on the polished/etched surface of sintered specimens for both AC and BC. No marked difference was observed in these microstructures such in the size, size distribution and morphology of grains. The microstructures were uniform without excessively large and/or agglomerated grains.

Fig. 4 shows the SEM micrograph taken with low magnification for the sintered specimen of the AC group. Spherical and crack-like pores were found to be distributed throughout the system. Similar pore structure was observed in the BC specimen. The size of pores ranged from several to several tens of micrometers.

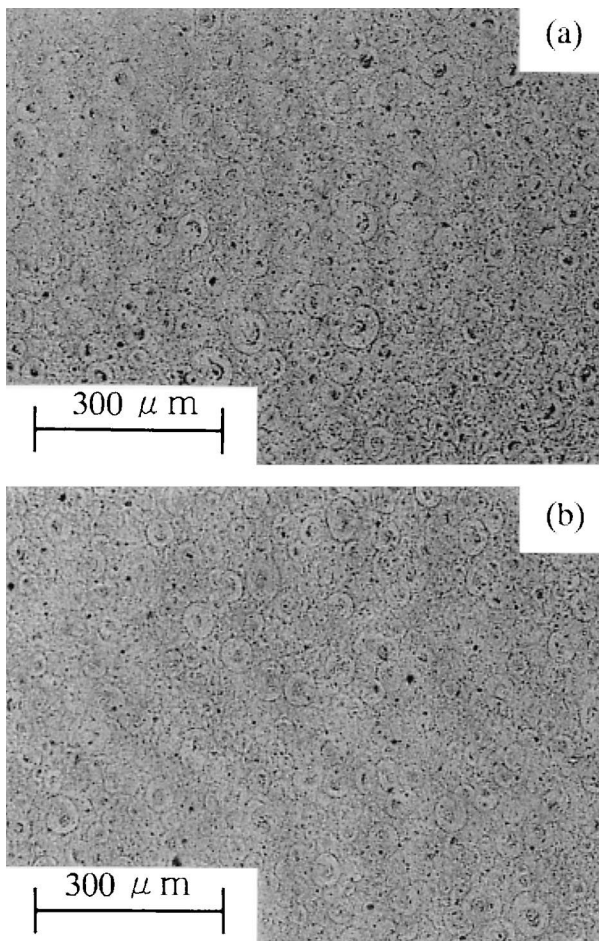


Fig. 2. Internal structure of green bodies made through (a) AC and (b) BC processes.

Fig. 5 shows the photomicrographs taken with transmission mode on thinned specimens in both the AC and BC groups. The trace of granules are visible for both specimens even after sintering. Many pores are noted again at the center and between the trace of granules. Those pores should be identical to pores or void spaces found in the SEM micrograph shown in Fig. 4. Clearly, the pores found in green bodies persisted at least partially during the densification process. The pore size is larger for the sample AC than for BC as observed in green compacts (Fig. 2). Conventional characterization tools such as SEM could not reveal such a minor difference in the pore structure. This successful identification can be ascribed again to the potential of the direct observation techniques.

For the present samples, sintered bulk densities were essentially the same regardless of the alteration of the procedure, showing 3.93 g/cm^3 for both AC and BC samples. Fracture toughness was $4.6 \text{ MPam}^{1/2}$ for both specimens and also the same. On the other hand, a clear difference was found in the fracture strength. Fig. 6 shows the Weibull distributions of the fracture strength measured for the specimens in both groups. Fracture strength of the BC specimens was clearly higher than that of AC. Average strength of the AC samples, 362 MPa, was in good coincidence with the results shown in the previous reports on the strength of sintered alumina that were made through the similar production route.^{4,5} On the other hand, the strength of BC samples was appreciably higher, 390 MPa. Weibull modulus was high for both groups, suggesting that the size of fracture origins was rather uniformly large.

Fig. 7 shows the relation between the concentration and the size of pores for AC and BC samples. The pore density was defined as the number of pore per unit volume of specimen per unit size interval. The analysis was carried out for specimens with the effective volume about 2.7 mm^3 by using the photomicrographs taken with transmission mode. For determination of the pore concentration, the number of pores was counted per pore size of $5 \mu\text{m}$ interval, and plotted on the figure as the intermediate value in the interval. A clear difference is noted in the figure, showing that the density of large pores is significantly higher in AC samples than in BC for the size range examined. The maximum size of defect found was approximately $60 \mu\text{m}$ for this examination volume.

The average fracture strengths measured on a single granule for both as-granulated and dewaxed granules were 0.29 and 0.41 MPa respectively. Dewaxed granules clearly exhibited higher fracture strength. Microscope observation of the tested granules revealed that both granules fractured fragily. The difference in fracture behavior was that the dewaxed granules broke into many small fragments by loading, whereas as-granulated ones split into several large and connected pieces.

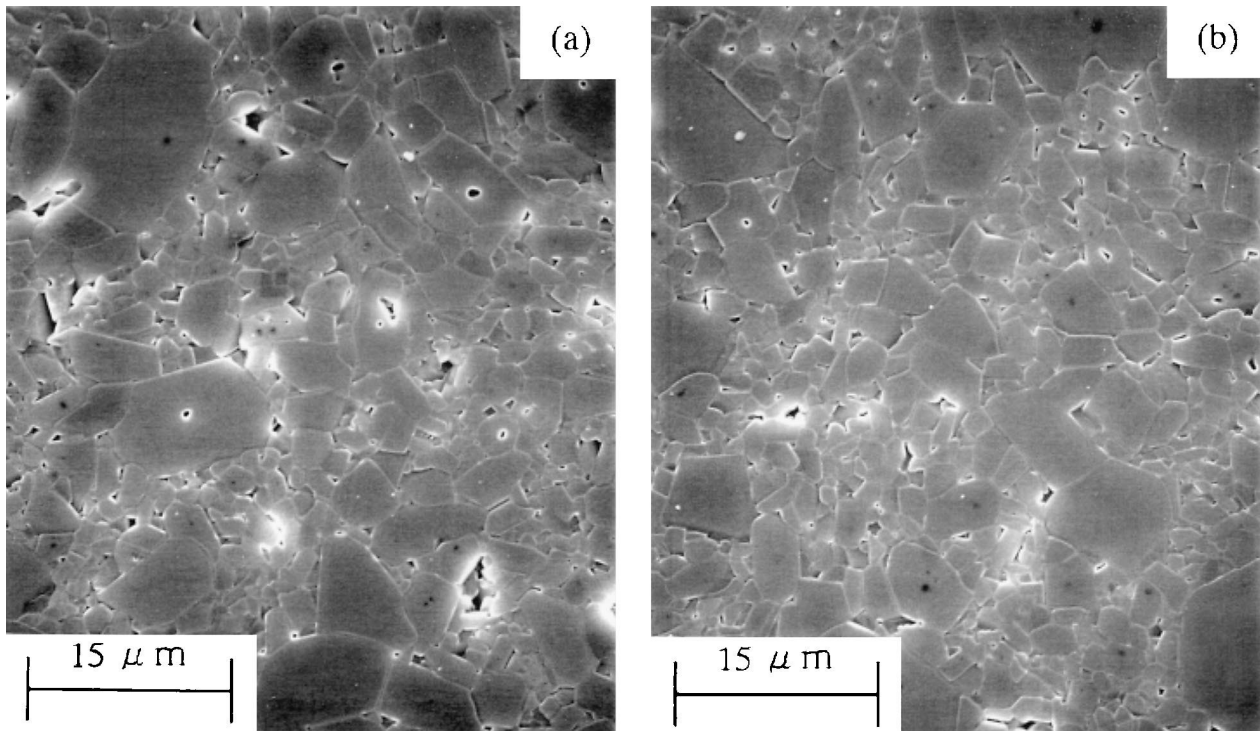


Fig. 3. Microstructure of sintered bodies made through (a) AC and (b) BC processes.

4. Discussion

This study has again clarified the influence of the minor difference of the structure in sintered ceramics on the mechanical strength quantitatively, as reported in the previous paper.⁵ Variation of the properties in ceramics with a minor change of processing condition can be detected by the conventional characterization tools such as density and strength measurements. It is, however, often very difficult to clarify the important factors exerting an influence on such a variation. The transmission characterization approach thus becomes crucial for understanding the results which are obtained by the conventional approach.

Variation of the strength in the present alumina ceramics should be related to the pore size distribution, especially of large pores with the size nearly 100 μm.^{5,7} As described above, the same sintered densities (3.93 g/cm³) were obtained for the samples in both groups. The same value of the density indicates that both samples contain the same pore volume. For ceramics, the strength–density relationship is given empirically as follows.¹⁹

$$\sigma = \sigma_0 \exp(-nP)$$

where, σ is the strength, σ_0 and n are constants, and P the porosity. The value of n changes from 4 to 7 for various kinds of ceramics. According to this relationship, ceramic materials with the same pore volume are

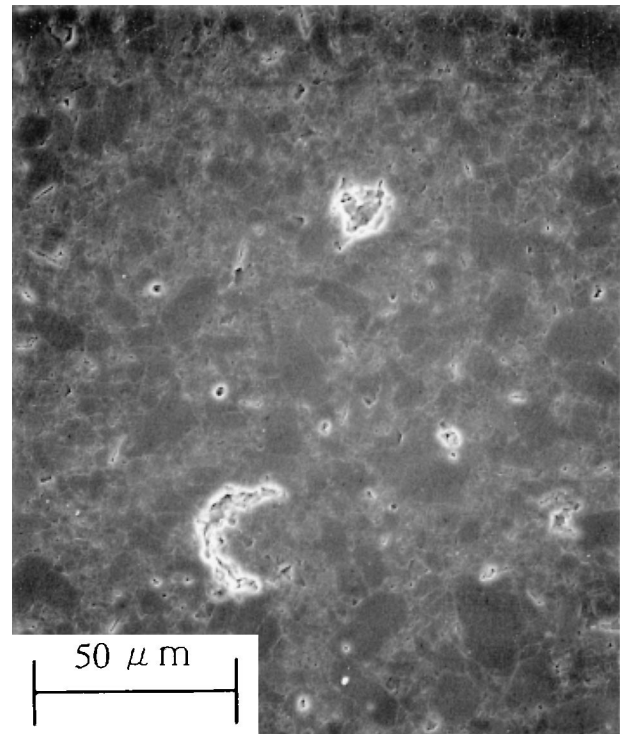


Fig. 4. Distribution of pore defects found in the polished/etched surface of the specimen AC by SEM.

expected to have nearly the same fracture strength, provided that they are prepared from the same powders through the similar production route. Difference in the strength for the present sintered alumina ceramics

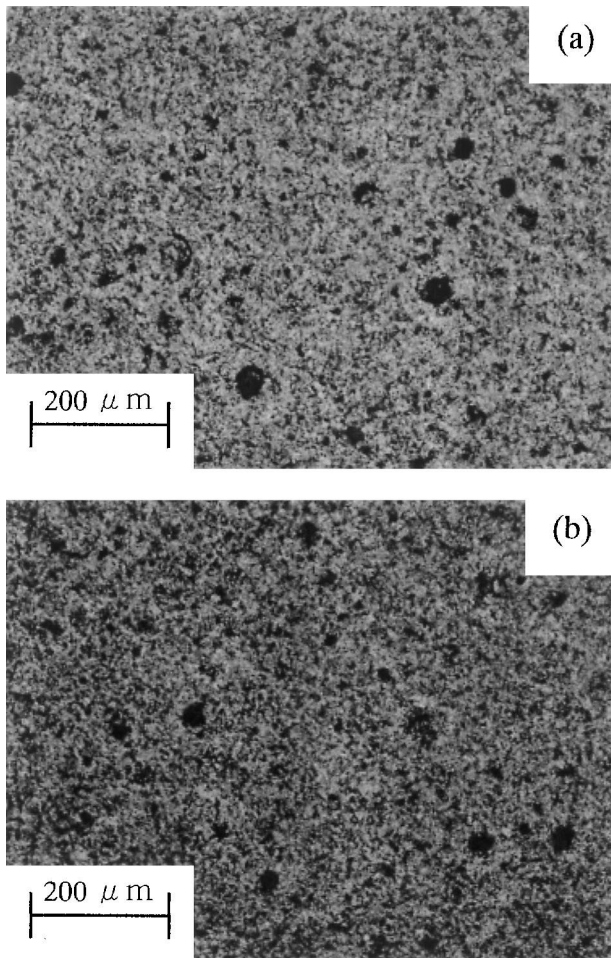


Fig. 5. Internal pore structure of sintered bodies made through (a) AC and (b) BC processes.

should, therefore, be explained in terms of the pore size distribution, not of the porosity. Direct observation revealed the slight change of the internal pore structure for the present materials as shown in Fig. 5. The apparent high concentration of pores for both AC and BC specimens does not contradict the high relative density (98.7% for the present samples) of the sintered bodies, because it can be ascribed to the unique observation method in which pores located at various depth in the specimen are observed simultaneously.

The difference of fracture strength can be explained by the difference of pore structure in sintered bodies. Notice the histogram of the pore density against the pore size shown in Fig. 7 that was determined from the photomicrographs taken for sintered specimens in transmission mode. A clear difference can be found in the defect size distribution between AC and BC samples. Variation of the strength for the present alumina ceramics can be explained quantitatively with this change of pore size distribution. Focused on large pores with the size nearly 100 μm , which should be expected to govern the fracture behavior of sintered bodies as

fracture origins, $0.02 \text{ mm}^{-3} \mu\text{m}^{-1}$ is nearly the concentration where the maximum pore size in the AC specimen becomes 100 μm , provided that the curve can be extrapolated to the region of such the large defects. At that concentration, Fig. 7 indicates that the size is 1.3 times larger for the AC specimen than for the BC. Provided that the shape factor of defects being the same, this difference in the defect size corresponds to 1.1 times higher strength for the BC specimen since the strength is inversely proportional to the one-half power of the size of fracture origin for specimens with the same fracture toughness. The result presented in Fig. 6 demonstrates that this estimate is in good agreement with the increase of fracture strength for the BC specimen, showing that the average strength of BC specimens (390 MPa) is 1.1 times higher than that of AC (362 MPa).

Influence of the pore structure on the variation of fracture strength is also obvious in the Weibull plot presented in Fig. 6. High Weibull modulus is noted for both samples, 22 for BC and 26 for AC. The result clearly shows that the alternative sources, such as inclusions or large grains developed through the abnormal grain growth, are unlikely to be the major fracture origins governing the strength of the present ceramics. High Weibull modulus and the parallel line in the plot can be explained by the high concentration of pores as fracture origins. A high concentration of pore defects with uniform distribution allows the number and size of pores, within the effective volume for fracture to be similar and makes the strength be rather constant for all tested specimens.

Pore structure in sintered bodies is influenced by the microstructure of green bodies. Pores at the middle and/or at the boundary of granules found in green compacts (Fig. 2) should be the major source of defects in sintered bodies, as mentioned in the past studies.^{5–9} Because it can be expected that the morphological change of pores with densification is similar for all the tested samples, smaller size of pores in the green compact of the BC group should be responsible for making the pore defect size be smaller in sintered body, resulting in the increase of fracture strength of BC samples. The result indicates that dewaxing of mold pressed powder compacts before CIP by the heat-treatment was effective in reducing the pore size in green compact.

Formation of large pores during the forming process depends on the characteristics and compaction behavior of granules. It has been reported that soft granules are required to promote the uniform powder packing with complete joining at their boundaries and to achieve high green density with small pore size.^{12–17} Another previous report also suggests that the heat-treatment of granules results in the strengthening of granules due to the neck growth between primary particles and is, therefore, detrimental for the reduction of void spaces between granules.²⁰ Even in the present study, heat-treated

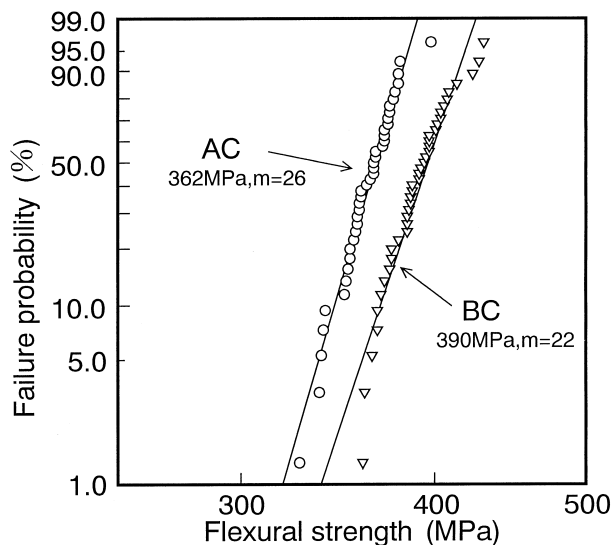


Fig. 6. Weibull distributions of the fracture strength measured for the specimens made through AC and BC processes.

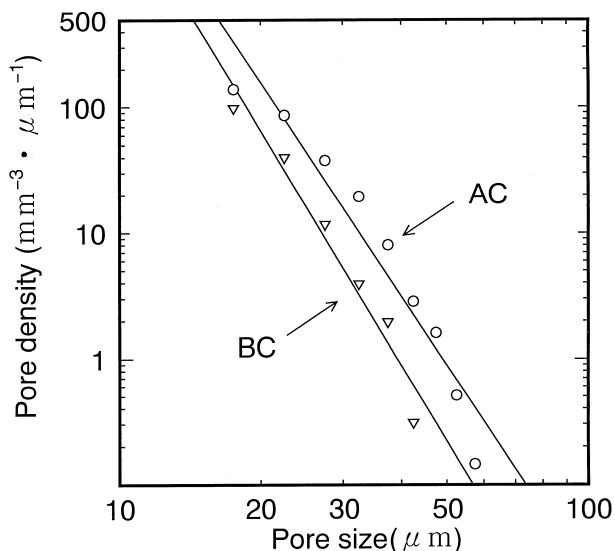


Fig. 7. Relation between the concentration and the size of pores for AC and BC samples.

granules exhibited higher strength (0.41 MPa) than that of as-granulated ones (0.29 MPa). The result suggests that the dewaxing of powder compacts before CIP should be detrimental for the promotion of uniform powder packing because the compaction during CIP is still governed by the characteristics of granules. It is thus, interesting that the sintered bodies in the BC group contained smaller pore defects and exhibited higher strength.

Difference of fracture behavior between as-granulated and dewaxed granules should be the key to solving that problem. Hard granules should be useful to promote the uniform packing during consolidation at the initial stage of compaction, because of the effective pressure

transmission to the inside. Fragmentation of granules into small pieces, after the initial promoted packing, would be favorable to fill the voids in and between granules and to promote uniform powder packing with small pores throughout the system. As described above, both granules fractured fragilely in the present case. The difference was the fracture behavior. Dewaxed granules broke into many small fragments by loading, whereas as-granulated ones only split into several large and connected pieces. Such the difference in the fracture behavior of dewaxed granules was considered to result in the reduction of void spaces in BC samples during consolidation by CIP. Details of the effect of heat-treatment of granules on the fracture behavior are still under examination and will be discussed in the other extensive paper.

5. Conclusion

Dewaxing before CIP with the heat-treatment of powder compacts was effective to make the pore defect size in green and sintered bodies be small and to improve the fracture strength of sintered bodies. Reduction of pore size in green compact was ascribed to the promotion of rather uniform powder packing for heat-treated and dewaxed granules. It was considered that brittle fracture of the granules into many small fragments after the effective pressure transmission was responsible for the reduction of pore size in green bodies by filling the void spaces with powder particles during consolidation by CIP.

References

1. Takahashi, H., Shinohara, N., Uematsu, K. and Tsubaki, J., Influence of granule character and compaction on the mechanical properties of sintered silicon nitride. *J. Am. Ceram. Soc.*, 1996, **79**, 843–848.
2. Iwamoto, Y., Nomura, H., Sugiura, I., Tsubaki, J., Takahashi, H., Ishikawa, K., Shinohara, N., Okumiya, M., Yamada, T., Kamiya, H. and Uematsu, K., Microstructure evolution and mechanical strength of silicon nitride ceramics. *J. Mat. Res.*, 1994, **9**, 1208–1213.
3. Takahashi, H., Shinohara, N., Okumiya, M., Uematsu, K., Iwamoto, Y., Tsubaki, J. and Kamiya, H., Influence of slurry flocculation on the character and compaction of spray-dried silicon nitride granules. *J. Am. Ceram. Soc.*, 1995, **78**, 903–908.
4. Shinohara, N., Okumiya, M., Hotta, T., Nakahira, K., Naito, M. and Uematsu, K., Effect of seasons on density, strength of alumina. *Am. Ceram. Soc. Bull.*, 1999, **78**, 81–84.
5. Shinohara, N., Okumiya, M., Hotta, T., Nakahira, K., Naito, M. and Uematsu, K., Seasonal variation of microstructure and sintered strength of dry-pressed alumina. *J. Am. Ceram. Soc.*, in press.
6. Hotta, T., Nakahira, K., Naito, M., Shinohara, N., Okumiya, M. and Uematsu, K., Origin of strength change in ceramics associated with the alteration of spray dryer. *J. Mater. Res.*, 1999, **14**, 2974–2979.
7. Shinohara, N., Okumiya, M., Hotta, T., Nakahira, K., Naito, M. and Uematsu, K., Formation mechanisms of processing defects

- and their relevance to the strength in alumina ceramics made by powder compaction process, *J. Mater. Sci.*, in press.
8. Zhang, Y., Inoue, M., Uchida, N. and Uematsu, K., Characterization of processing pores and their relevance to the strength in alumina ceramics. *J. Mater. Res.*, 1999, **34**, 4271–4277.
 9. Uematsu, K., Sekiguchi, M., Kim, J.-Y., Saito, K., Mutoh, Y., Inoue, M. and Fujino, Y., Effect of processing conditions on the characteristics of pores in hot isostatically pressed alumina. *J. Mater. Sci.*, 1993, **28**, 1788–1792.
 10. Uematsu, K., Miyashita, M., Kim, J.-Y., Kato, Z. and Uchida, N., Effect of forming pressure on the internal structure of alumina green bodies examined with immersion liquid technique. *J. Am. Ceram. Soc.*, 1991, **74**, 2170–2174.
 11. Uematsu, K., Immersion microscopy for detailed characterization of defects in ceramic powders and green bodies. *Powder Technology*, 1996, **88**, 291–298.
 12. Nies, C. W. and Messing, G. L., Effect of glass-transition temperature of polyethylene glycol-plasticized polyvinyl alcohol on granule compaction. *J. Am. Ceram. Soc.*, 1984, **67**, 301–304.
 13. Frey, R. G. and Halloran, J. W., Compaction behavior of spray-dried alumina. *J. Am. Ceram. Soc.*, 1984, **67**, 199–203.
 14. Dimilia, R. A. and Reed, J. S., Dependence of compaction on the glass transition temperature of the binder phase. *Am. Ceram. Soc. Bull.*, 1983, **62**, 484–488.
 15. Tanaka, H., Fukai, S., Uchida, N. and Uematsu, K., Effect of moisture on the structure and fracture strength of ceramic green bodies. *J. Am. Ceram. Soc.*, 1994, **77**, 3077–3080.
 16. Youshaw, R. A. and Halloran, J. M., Compaction of spray-dried granules. *Am. Ceram. Soc. Bull.*, 1982, **61**, 227–230.
 17. Zheng, J., Reed, J.S., Particle and granule parameters affecting compaction efficiency in dry pressing. *J. Am. Ceram. Soc.*, 1988, **71**, C-456–C-458.
 18. Naito, M., Nakahira, K., Hotta, T., Ito, A., Yokoyama, T. and Kamiya, H., Microscopic analysis on the consolidation process of granule beds. *Powder Technology*, 1998, **95**, 214–219.
 19. Kingery, W. D., Bowen, H. K. and Uhlman, D. R., *Introduction to Ceramics (2nd ed.)*, John Wiley and Sons, New York, 1976, pp. 768–815.
 20. Lukasiewicz, S. J. and Reed, J. S., Character and compaction response of spray-dried agglomerates. *Am. Ceram. Soc. Bull.*, 1978, **57**, 798–801.